LOCATION OF THE CARBOXYL TERMINUS OF BACTERIORHODOPSIN IN PURPLE MEMBRANE

B. A. WALLACE AND R. HENDERSON
MRC Lab of Molecular Biology, Cambridge, England

ABSTRACT Purple membrane samples have been prepared by trypsin digestion to have either 10 or 21 residues removed from the carboxyl terminus of the proteins. Electron diffraction of single membranes and x-ray diffraction of unoriented membrane pellets have been carried out on both these specimens and on native purple membranes. The main conclusion from this work is that the carboxyl terminus is almost entirely disordered, being free to take up many positions, and that its removal does not affect the packing in the crystal. The low resolution x-ray diffraction difference map may also suggest the approximate location of the carboxyl terminus.

INTRODUCTION

Bacteriorhodopsin is a light-driven proton pump that forms regular 2-dimensional arrays in the purple membrane of *Halobacterium halobium*. The protein consists of seven helical rods oriented perpendicularly to the membrane. Based on the three-dimensional map (1) and the amino acid sequence (2, 3), a model for the folding of the polypeptide chain has been proposed (4). To provide an experimental basis for verification of this or other possible models, we have modified the protein by labeling or proteolytic digestion, and used difference Fourier methods to locate the sites of modification in the crystal (5). When coupled with a knowledge of the chemistry of the modification, difference electron density maps can be used to determine the position of parts of the protein. One of the simpliest modifications is removal of a number of the carboxyl-terminal amino acids by proteolytic digestion. This paper describes the results of such an analysis.

METHODS

Purple membranes were prepared from *H. halobium* as described (6). Purple membrane concentration was estimated by ϵ_{570} (1 mg/ml, 1 cm) = 1.55 (7).

Digestion Conditions

Method I. 1 ml of a suspension of purple membrane (2 mg/ml in distilled H_2O) was treated with 0.25 mg porcine trypsin (Armour lot #K258256). The mixture was incubated at 18°C for 1 wk after which the sample was pelleted at 40,000 *g* and washed twice, each with 15 ml of distilled water. To ascertain that the clipped piece was actually removed and did not adhere to the membrane, the specimens were also washed with 1 M NaCl, followed by distilled water.

Method II. 2 mg of a suspension purple membrane in 1 ml of buffer (25 mM tris, 15 mM NaCl, 5 mM $CaCl_2$, pH 7.5) was treated with 0.05 mg porcine trypsin. The mixture was incubated at 18°C for 72 h, pelleted and washed twice with distilled water.

Gel Electrophoresis

The progress of the digestion, and molecular weights of the products were determined by electrophoresis in 15% polyacylamide gels containing 0.1% SDS as described by Laemmli (8). These were calibrated using ovalbumin, soybean trypsin inhibitor, lysozyme, and cytochrome *c* as standards.

Amino Acid Analysis

Digested and native samples were hydrolyzed in 6 M HCl containing 1% phenol for 24 h at 105°C and analyzed on a Durrum amino acid analyzer.

Sequence Fit

The site of cleavage was identified by comparing the amino acid analyses to the sequence using a simple computer program. The program fit the data by a correlation of measured amino acid content with the calculated composition that would be obtained by cleavage at each amino acid throughout the molecule. A residual factor $\{R_f = \Sigma_{i-1}^{n} | [N_i^o/N_i^p - 1] | \}$ was calculated for each possible cleavage site where i was for each amino acid type, N_i^o was the number of moles of each amino acid observed and N_i^p was the number of moles predicted. The minimum R_f value corresponds to the site of cleavage. As a test of the fit, the program was also run with idealized data for several different cleavage sites.

Electron Diffraction

Diffraction of unstained specimens in 0.5% glucose was done as described (9), using isolated single membrane patches of 1–2 μm diameter, which were tilted by <2.7° (as estimated from the ratios of intensities of symmetry related spots with known sensitivity to tilt, i.e., the 1,4 and 4,2 reflections). The average R factor[1] between Friedel pairs in six films was 19.8% for digest I and 21.8% for digest II. Diffraction patterns were scanned using a Joyce-Loebl mk4 micro-densitometer with a 10 μm

Dr. Wallace's address is the Department of Biochemistry, Columbia University, New York, N.Y. 10032. Address correspondence to B.A.W.

[1]The R-factor used here was $(\Sigma_{i-1}^{n} | I_i - I_T |)/[\Sigma_{i-1}^{n}(|I_i + I_T|/2)]$, where I_i and I_T are the intensities of a spot and its Fridel pair.

TABLE I
ELECTRON DIFFRACTION AMPLITUDE DIFFERENCES FOR DIGEST I AND DIGEST II SAMPLES AND NATIVE PHASES

h	k	F		
		Digest I	Digest II	Degrees
1	2	−0.22	0.70	312
1	4	−0.30	1.21	308
1	5	−0.12	−0.12	268
1	7	0.57	0.37	180
2	1	−1.40	−0.39	210
2	2	−0.52	−0.42	118
2	3	−1.40	1.11	342
2	4	−0.02	0.56	240
2	5	−0.21	−0.33	272
2	6	−1.36	−0.75	190
3	0	−0.57	−1.10	96
3	1	0.21	0.14	188
3	2	−0.22	0.39	5
3	3	1.40	−1.10	345
3	4	−0.85	−1.00	162
3	5	−0.10	1.99	300
4	0	0.26	−0.55	282
4	1	1.08	0.63	318
4	2	0.58	−0.09	103
4	4	0.60	−0.88	241
5	0	−0.13	−0.44	345
5	1	1.30	−1.12	28
5	2	−0.62	−0.52	130
5	3	1.14	−0.95	185
6	0	1.40	−1.19	329
6	1	−0.69	0.47	0
6	2	0.28	−0.27	320
7	0	−0.45	−1.26	260
7	1	0.26	−0.79	257

circular aperature. Symmetry-related reflections were averaged, and a least-squares scaling of six native and six derivative films was done to minimize their differences. Projection maps were calculated from the (native minus derivative) amplitudes and native phases, (Table I) using a Fourier program written by G. Reeke. The rms values of $(\Delta F/F)$ for the digest I and II maps were 1.72% and 2.78%, respectively. An indication of the reproducibility, or noise levels, is that similar calculations on two sets of native data, which gave rms $(\Delta F/F)$ values of ~1.4–1.7%.

X-ray Diffraction

Diffraction of concentrated unoriented specimens in distilled H_2O was done as described (10). The diffraction patterns were circularly averaged over the two most intense 60° arcs. The ratio of the native over the digested intensities was plotted vs. the radius of the reflection. Although unoriented patterns also contain contributions from each lattice line, at this resolution, the off-equitorial parts of the lattice lines are at higher radii than the radius at which the center of the line occurs and so no significant error is introduced by using the intensities from the powder pattern. At higher resolution the difference in radius would become significant.

Since the (1, 2) and (2, 1) reflections are coincident in the x-ray diffraction, it is necessary to assign the intensity contribution to each reflection, in order to calculate a map. It was assumed that the x-ray intensities would be in approximately the same ratio (4.3) as the electron intensities, so the intensity of the (1, 2) was taken as 0.81 times the observed intensity difference. A low resolution difference Fourier map (native minus derivative) was calculated using the average structure factors of the (1, 0), (1, 1), (2, 0), and (1, 2) reflections, whose values were +43.0, +168.0, +82.0, and +39.0, respectively, and the phases obtained from electron microscopy images of native purple membranes (9).

RESULTS

Gel electrophoresis studies indicated that a single major protein band, with a slightly smaller molecular weight than the native protein, remains associated with the membrane after proteolysis (Fig. 1 *a*) using methods I and II. The digestion conditions did not result in any internal sites of cleavage, so the soluble material removed must have been either from the NH_2- or COOH-terminus. Using calibration standards, it was possible to estimate the amount of material lost upon digestion to be 800 and 2,300 daltons for digest I and II conditions, respectively (Fig. 1 *b*). These estimates are approximate, because even native bacteriorhodopsin from polyacryamide gel electrophoresis in SDS was estimated to be 21,000, whereas the actual value is 26,500. Values for bacteriorhodopsin ranging between 19,000 and 26,000 have been reported in different gel systems (11–14).

To determine where the sites of cleavage were, amino acid analyses of digest I and II specimens were done. Because the detection and recovery of all amino acid types are not equivalent, these were standardized against a native sample, whose actual amino acid composition is known from the complete sequence determination. A computer program was used to correlate the digest compositions with all possible cleavage sites, by sequentially removing one amino acid at either end of the molecule, calculating the composition, and then comparing it with the experimental values. The best fits to the data were found to be 10 and 21 amino acids missing from the COOH-terminus for digest I and II, respectively (Fig. 2). These compared well with calculated fits to the data (see test data, Fig. 2) when experimental composition values were set at 10 and 21 amino acids deleted from the

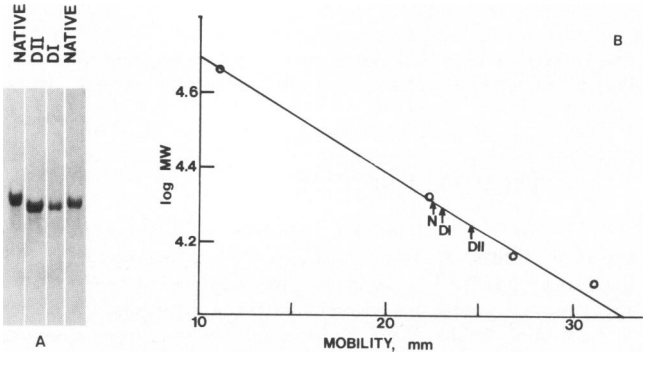

FIGURE 1 (*a*) SDS polyacrylamide gel of native, digest I (DI), and digest II (DII) purple membrane samples. (*b*) Molecular weight calibration plot of SDS gel. The migration distances of the molecular weight (MW) standards (O), digest I and digest II, and native (N) samples are indicated. Apparent losses of ~800 and ~2,300 daltons, respectively, are obtained upon proteolysis using methods I and II.

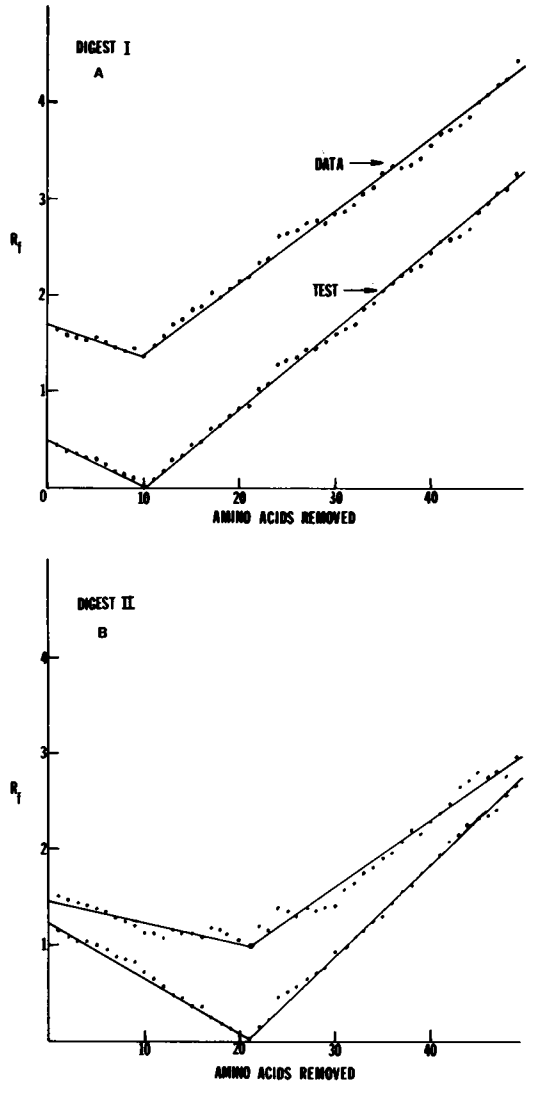

FIGURE 2 Plots of computer fit of R_f vs. number of amino acids removed, showing both ideal test data and experimental values for (*a*) digest I (10 amino acids removed) and (*b*) digest II (21 amino acids removed).

COOH-terminus, and the same correlation program run. Removal of 10 or 21 amino acids would cause losses in molecular weight of 788 or 1,933, which are within experimental error of the observed SDS-PAGE values.

Digestion conditions that limited aggregation of the membranes were used. The carboxyl terminus has a large negative charge, which may provide a means of repelling other membranes; once this has been removed, the membrane cytoplasmic surfaces tend to adhere to one another. A number of other digestion conditions were tested (e.g., in this same buffer with 0.25 mg of trypsin for 3 h at 37°C), which resulted in membranes sticking together and digestion of only a portion of the samples, as seen on SDS gels. In addition, it was noted, based on SDS-PAGE gels, that substantially older specimens (i.e., 1–5 yr) stored at 4°C in distilled H_2O or sucrose solutions that contained azide, also often had 10 amino acids missing.

The samples produced by methods I and II were subjected to electron diffraction analyses in order to identify the location of the carboxyl terminus in the physical map. For each Fourier difference map, six native and six derivative data sets, to which temperature factor corrections had been applied, were scaled and averaged in order to limit the contributions of random variations between samples. Since each pattern contains six hexagonally related spots in projection, this means that the native and derivative reflections were each measured 36 times and averaged. Variation between electron diffraction patterns of identical specimens is greater than between x-ray diffraction patterns because interactions of the sample with the substrate (carbon grid) may distort the lattices. Also, radiation damage and variation in glucose embedding may produce other systematic errors. The size of the patches of ordered arrays and the degree of preservation of order upon drying are further significant factors in the quality and extent of resolution of the films. Since the Fourier map is dependent upon accurate phasing, and reliable native phases to 7 Å were available from images, difference maps were calculated at this resolution, although the diffraction spots extended beyond 6 Å.

Some of the most intense reflections were not included in the calculated map. On films that were sufficiently exposed to permit accurate measurement of the weaker, high resolution spots, the optical densities of these more intense spots did not fall within the linear range of the photographic recording material and were excluded from the data sets.

Two independent maps were calculated for each derivative using six different native and six derivative data sets. In both maps, the strongest features were present in the same region, although secondary peaks were altered in position and intensity for the different sets of data.

It was anticipated that if the proteolytic cleavages did not disrupt the lattices or cause a major change in protein conformation, then the carboxyl terminus should appear as a positive peak in the (native minus digested) difference Fourier maps.

The helix nomenclature used here is the same as indicated in Engelman, et al. (4), letters A–G referring to the helical regions in the sequences, and numbers 1–7 to the rod-shaped features in the physical map.

The initial observation for the data was that the total ΔF was very small. The calculated ΔF for the digest I sample, if all the residues were well-ordered in the crystal but not necessarily all concentrated at one position, is at least 7.7% (calculated for the "worst" case with density distributed over the entire unit cell). Even if all of that ΔF measured (1.72%) is real (i.e., not the result of error in measurement), the maximum number of equivalent carbon atoms that could be contributing to the difference Fourier would be four, or about one amino acid. In actuality, the errors in measurement (between two native data sets) are on the order of 1.4–1.7%, so less than one amino acid in the di-

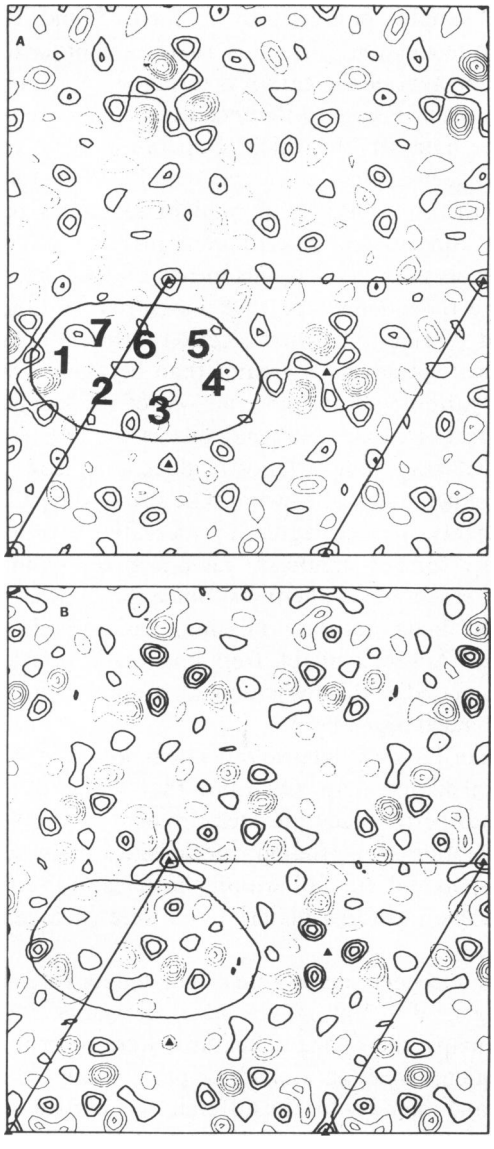

FIGURE 3 Electron diffraction difference maps produced from an average of six native minus six derivative films for the (*a*) digest I and (*b*) digest II samples. The approximate boundary of the seven helices of the bacteriorhodopsin molecule is outlined by the ellipse and the unit cell of the crystal (63 Å) is indicated.

gest I sample may be ordered. For the digest II sample, this would suggest that approximately one amino acid was ordered. In the difference electron density map for digest I (Fig. 3 *a*), only one group of peaks slightly above noise is seen at the left side of the molecular boundary near one of the threefold axes, and in the area of helices 1 and 2. The presence of alternating positive and negative peaks in this region suggests a rearrangement (small) of either lipid or protein components. In the difference Fourier map for the digest II sample, there is also no clear evidence of loss of ordered diffracting material, but again peaks in the map suggest that motion of a portion of the molecule has occurred upon removal of the COOH-terminus. The general location of the features, although slightly different from those in the digest I map, is also near the threefold axis, close to helices 1 and 2 (Fig. 3 *b*). No such features were found in (native minus native) maps.

Because these results suggest the COOH-terminus is located near helices 1 and 2 on the left side of the molecule, there should be less material present in that portion of the crystal after digestion. It was therefore predicted that there should be additional penetration of heavy metal stains near the adjacent threefold axis in images of negatively stained membranes. Images of uranyl acetate-stained specimens were examined and a low-resolution electron density map was calculated (data not shown). Additional stain was usually present in that region, consistent with the unstained diffraction data, but the variation between images of different areas of the same grid was as great as the anticipated differences in staining.

Since the COOH-terminus appeared, from the electron diffraction experiments, to be disordered, x-ray diffraction studies were done in order to clearly locate the 21 amino acids which must contribute to the total scattering power of the membranes. It was expected that since the low resolution reflections are responsible for the difference in contrast between protein and lipid, removal of protein mass, whether it is well-ordered or not, should result in a reduction in their intensity, while the higher resolution reflections resulting from well-ordered features, would, as in the electron-diffraction experiments, be unchanged upon removal of the COOH-terminus. Circularly averaged densitometer plots of x-ray diffraction patterns of native and digest II samples are shown in Fig. 4. The low-resolution reflections of the native sample are more intense, relative to the digested samples, than the higher resolution spots (Fig. 5). The intensities of the (1, 0), (1, 1), (2, 0), and (1, 2) reflections of the native were larger than digest I by factors of 1.09, 1.23, 1.10, and 1.10, respectively, while for digest II, the values were 1.13, 1.186, 1.156, and 1.101.

In order for the x-ray diffraction results obtained to be meaningful, it must be shown that the degree of ordering (orientation) of the native and digested samples is nearly the same. Since the Lorentz factor is proportional to r^2 (where r is the radius of the ring in the diffraction pattern) for an unoriented dispersion and proportional to r in a completely oriented (parallel stacked membranes) specimen, the ratio of these factors is proportional to r. There-

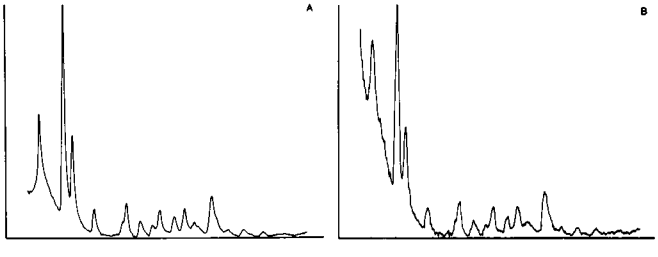

FIGURE 4 Densitometer scans of circularly averaged x-ray diffraction patterns of (*a*) native and (*b*) digest II samples. The digest II sample was slightly more dilute, and hence the higher noise level.

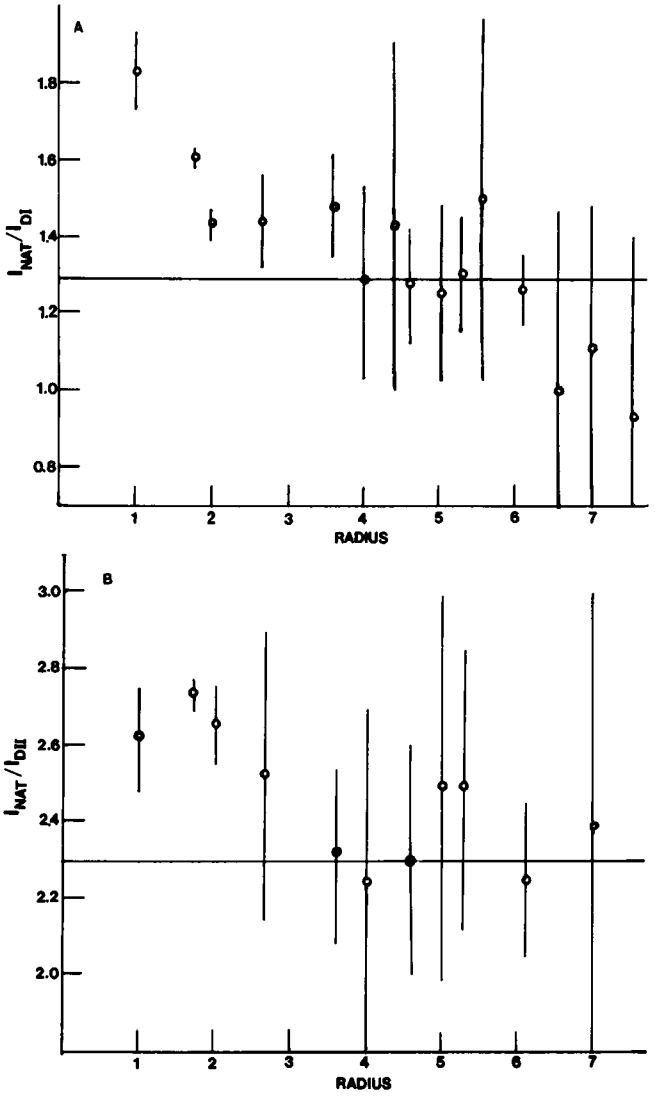

FIGURE 5 Plot of the log of the ratios of native x-ray intensities to the digested x-ray intensities vs. radius of the reflections for (*a*) digest I and (*b*) digest II samples. Error bars were derived from the noise levels in regions between peaks in the densitometer scans (see Fig. 4).

fore, if one sample was slightly more ordered than another, the ratio plotted against the radius (Fig. 5) would give a sloping line rather than a straight line with the low resolution reflections displaced in much the same way as is observed.

To test whether the specimens were oriented, one can examine the diffraction patterns to see whether the intensity of the rings deviates from being circularly symmetric. By eye, all patterns appeared to be almost completely symmetrical, although the native may, if anything, have been slightly more ordered (asymmetric) than the digested. This observation was confirmed by a comparison of the integrated intensities of different 60° sectors in each diffraction pattern: the digested patterns were of nearly uniform intensity throughout, while the native varied somewhat with angular displacement. This indicates any slope of the ratio plot should be positive. While it is possible to draw a negatively sloped line through the data, using the extremes of the experimental errors, this is not consistent with the orientation data. The correct plot must therefore be essentially independent of r and the 9–23% differences in the low-resolution peaks observed must be real and not due to an ordering effect. If anything, the differences would be larger than those observed. A low-resolution difference Fourier map using the (1, 0), (1, 1), (2, 0), and (2, 1) reflections was then calculated using the differences obtained by averaging the digest I and II data. Since the error bars for each of the measurements shown in Fig. 5 is quite high, this averaging procedure should produce more reliable differences than for each of the sets of data alone although the values were very similar. In the (native minus digest) map (Fig. 6), a positive peak should indicate the location of the COOH-terminus. A peak is indeed observed in a position near the features in the electron diffraction map. Given the much lower resolution of this x-ray difference map, and considering that different parts of the protein are being shown up, the two results are in reasonable agreement.

DISCUSSION

The digestion conditions utilized in this work result in single high molecular weight membrane-associated fragments. The site of trypsin cleavage under low ionic strength conditions (digest I), a Pro—Ser bond, is very unusual. Since relatively high concentrations of the enzyme have been used, proteolysis at this site may be due to an impurity, although this possibility is somewhat mitigated against because material from another supplier (Miles Laboratories, Elkhart, IN) also resulted in the same site of cleavage (plus a number of minor internal sites, possibly due to additional contaminants). Perhaps the folding of the

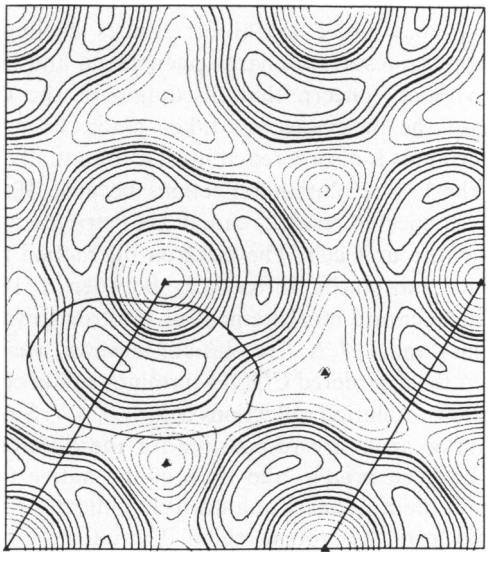

FIGURE 6 Low-resolution x-ray diffraction difference map calculated with data obtained by averaging the digest I and digest II data and synthesis of a Fourier map with coefficients indicated.

protein in the membrane, and the charge distribution at the surface are such that this pro-ser bond is the most accessible site in the molecule, and hence the apparently unusual specificity.

Electron diffraction of native and digested specimens of bacteriorhodopsin indicates that the COOH-terminus of the molecule is disordered in purple membranes. The observed ΔF, even for digest II is only 2.78%. This suggests that the maximum number of ordered or mostly ordered residues is approximately one (ΔF calculated for a single amino acid is ~2.5%). Furthermore, the electron diffraction difference maps for both 10 and 21 amino acids removed show no positive peaks significantly above noise, but do suggest small rearrangements of the protein upon removal of the COOH-terminus. This may be either a physical or charge-induced structural rearrangement resulting from the loss of not only nearly 10% of the total protein mass, but also the removal of four negative charges. It is suggested that the peaks indicate motion of the region of the polypeptide chain immediately adjacent in the sequence to the removed residues. These diffraction results suggest that the COOH-terminus may be located in the corner of the molecule occupied by helices 1 and 2, but since the peaks are weak, this alone is not conclusive evidence. It is clear, however, that not only is the COOH-terminus disordered, but its presence is not necessary for maintenance of the purple membrane structure in the native crystal. Upon removal, there is no change in the lattice constants, extent of order, nor any significant conformational change in the protein. It does, however, have a significant effect on the charge of the molecule, and removal eliminates the mutual repulsion of cytoplasmic surfaces of the purple membranes and hence digested specimens may tend to adhere with their cytoplasmic faces together, and form rather large clumps of precipitates, unless care is taken in the handling. This method of preparation may prove useful for studies dealing with purple membrane surface charge phenomena and may be utilized without concern that disruption of the overall structure of the molecules has taken place. Even if the COOH-terminus is disordered, it must differentially affect some of the low resolution reflections because 10 to 21 covalently connected residues cannot be distributed evenly throughout the unit cell. The electron diffraction results indicate no substantial differences between $1/18$ $Å^{-1}$ (where the accurate measurement of electron diffraction data begins) and $1/7$ $Å^{-1}$ resolution; however, we would expect that the disordered COOH-terminus would contribute to the low resolution reflections below $1/18$ $Å^{-1}$. Since the low resolution spots are responsible for the difference in contrast between protein and lipid in the native map, a reduction in their intensity qualitatively indicates removal of material from the protein region. The intensities of the low resolution (up to $1/20$ $Å^{-1}$) reflections were observed by x-ray diffraction to decrease upon removal of the COOH-terminus. The difference map shows the position of the material in a more quantitative way, but still at low resolution. The maximum of the peak is localized towards the same side of the protein (nearest helices 1 and 2) as the features in the electron diffraction difference maps. Thus the analysis by x-ray diffraction at low resolution and electron diffraction at higher resolution produce compatible results. Further more, since the x-ray studies were done using hydrated samples, this suggests the absence of water and presence of glucose in the electron diffraction studies was not responsible for structural rearrangements resulting in peaks in this region.

We publish these results because (*a*) the methods of both x-ray and electron diffraction analyses may be useful for other studies of the localization of particular modifications, (*b*) the proteolytic conditions may be useful for studies of surface charges, and (*c*) the results, although only suggesting a position for the carboxyl terminus, do indicate that it is almost completely disordered.

An important question still remains as to what the role of the carboxyl terminus is and why the organism expends biosynthetic energy to produce the 21 COOH-terminal amino acids. Besides being disordered in the native membrane and apparently unimportant for protein-protein interactions (the two-dimensional crystals are not at all disrupted when it is removed) it also appears to be unnecessary for proton-pumping activity (14), although it may have a role in pumping efficiency (15). It does impart a large negative charge to one surface of the molecule, which causes the isolated native membranes to repell one another, while the digested specimens tend to adhere face-to-face. However, this cannot be its role in vivo. It is possible that the carboxyl terminus is involved in the biosynthetic insertion of the protein into the membrane.

In summary, using electron and x-ray diffraction, we have shown that the 21 carboxyl terminal amino acids of bacteriorhodopsin which are susceptible to cleavage by trypsin, are generally disordered in the native two-dimensional crystalline purple membranes embedded in glucose. However, in the high salt concentrations that exist in vivo, the carboxyl terminus may be more precisely positioned. We also present evidence to indicate this portion of the molecule is localized near one particular region of the molecule. The difference Fourier maps suggest the carboxyl terminal helix(*G*) of the molecule is likely to be helix 2 in the projection map. This begins to align the folding of the polypeptide chain in the map and is consistent with the model we previously proposed (4).

We thank K. Edwards for running the amino acid analyses.

This work was supported by a grant from the Jane Coffin Childs Memorial Fund for Medical Research to B. A. Wallace.

Received for publication 2 November 1981 and in revised form 10 March 1982.

REFERENCES

1. Henderson, R., and P. N. T. Unwin. 1975. Three-dimensional model of purple membrane obtained by electron microscopy. *Nature* (*Lond.*). 275:28–32.
2. Ovchinnikov, Yu. A., N. G. Abdulaev, M. Yu, Feigina, A. V. Kiselev, and N. A. Lobanov. 1979. The structural basis of the functioning of bacteriorhodopsin. An overview. *FEBS* (*Fed. Eur. Biochem. Soc.*) *Lett.* 100:219–224.
3. Khorana, H. G., G. E. Gerber, W. C. Herlihy, C. P. Gray, R. J. Anderegg, K. Nihei, and K. Biemann. 1979. Amino acid sequence of bacteriorhodopsin. *Proc. Natl. Acad. Sci. U. S. A.* 76:5046.
4. Engelman, D. M., R. Henderson, A. McLachlan, and B. A. Wallace. 1980. The path of the polypeptide of bacteriorhodopsin. *Proc. Natl. Acad. Sci. U.S.A.* 77:2023–2027.
5. Wallace, B. A., and R. Henderson. 1980. Electron Microscopy at Molecular Dimensions. W. Baumeister and W. Vogell, editors. Springer-Verlag, Berlin. 57–60.
6. Oesterhelt, D., and W. Stoeckenius. 1974. Isolation of the cell membrane of *Halobacterium halobium* and its fractionating into red and purple membrane. *Meth. Enzymol.* 31:667–687.
7. Fisher, K. A., K. Yanagimoto, and W. Stoeckenius. 1978. Oriented absorption of purple membrane to cationic surfaces. *J. Cell Biol.* 77:611–621.
8. Laemmli, U. K. 1970. Cleavage of structural proteins during the assembly of the head of bacteriophage T4. *Nature* (*Lond.*). 277:680–685.
9. Unwin, P. N. T., and R. Henderson. 1975. Molecular structure determination by electron microscopy of unstained specimens. *J. Mol. Biol.* 94:425–440.
10. Henderson, R. 1975. The structure of purple membrane from *Halobacterium halobium*. Analysis of the x-ray diffraction pattern. *J. Mol. Biol.* 93:123–138.
11. Oesterhelt, D., and W. Stoeckenius. 1971. Rhodopsin-like protein from the purple membrane of *Halobacterim halobium*. *Nat. New Biol.* 233:149–152.
12. Bridgen, J., and I. D. Walker. 1976. Photoreceptor protein from the purple membrane of *Halobacterium halobium*. Molecular weight and retinal binding site. *Biochemistry*. 15:792–798.
13. Gerber, G. E., C. Gray, D. Wildenauer, and H. G. Khorana. Orientation of bacteriorhodopsin in *Halobacterium halobium* as studied by selective proteolysis. *Proc. Natl. Acad. Sci. U. S. A.* 74:5426–5430.
14. Abdulaev, N. G., M. Yu. Feigina, A. V. Kiselev, Yu. A. Ovchinnikov, L. A. Drachev, A. D. Kaulen, L. V. Khitrina, and V. P. Skulachev. 1978. Products of limited proteolysis of bacteriorhodopsin generate a membrane potential. *FEBS* (*Fed. Eur. Biochem. Soc.*) *Lett.* 90:190–194.
15. Govinjee, R., K. Ohno, and T. G. Ebrey. 1982. Effect of the Removal of the COOH-terminal Region of bacteriorhodopsin on its light-induced H^+ changes. *Biophys. J.* 38:82–85.